

# Supporting Information

---

## Design of self-cleanable multilevel anticounterfeiting interface through covalent chemical modulation

Manideepa Dhar,<sup>a,‡</sup> Ufuoma I. Kara,<sup>b,‡</sup> Supriya Das,<sup>a</sup> Yang Xu,<sup>b</sup> Sohini Mandal,<sup>a</sup> Robert L. Dupont,<sup>b</sup> Eric C. Boerner,<sup>b</sup> Boyuan Chen,<sup>b</sup> Yuxing Yao,<sup>c</sup> Xiaoguang Wang,<sup>b,d\*</sup> Uttam Manna<sup>a,e,f\*</sup>

<sup>a</sup> Bio-Inspired Polymeric Materials Lab, Department of Chemistry, Indian Institute of Technology-Guwahati, Kamrup, Assam 781039, India  
E-mail: [umanna@iitg.ac.in](mailto:umanna@iitg.ac.in)

<sup>b</sup> William G. Lowrie Department of Chemical and Biomolecular Engineering  
The Ohio State University, Columbus, OH 43210, USA  
E-mail: [wang.12206@osu.edu](mailto:wang.12206@osu.edu)

<sup>c</sup> Division of Chemistry and Chemical Engineering, California Institute of Technology, Pasadena, CA, 91125, USA

<sup>d</sup> Sustainability Institute, The Ohio State University, Columbus, OH 43210, USA

<sup>e</sup> Centre for Nanotechnology, Indian Institute of Technology Guwahati, Kamrup, Assam 781039, India

<sup>f</sup> Centre for Nanotechnology, School of Health Science and Technology, Indian Institute of Technology Guwahati, Kamrup, Assam 781039, India

### Experimental Section

#### Materials

Branched poly(ethyleneimine) (BPEI; molecular weight ~ 25,000 Da), dipentaerythritol penta acrylate (5-Acl), 2-hydroxy acrylate (HA), hexyl acrylate (HLA), octadecyl amine (ODA), and methylene blue were purchased from Sigma-Aldrich, India. Glutaraldehyde (Glu; 25 % aqueous solution) was purchased from Merck, India. Glucamine was purchased from TCI, India. 1-Heptanol was purchased from Alfa-Aesar, India. Tetrahydrofuran (THF) was purchased from RANKEM, India. Microscope glass slides were obtained from Jain Scientific Glass Works, India.

#### General considerations

Contact angle measurements were conducted using a Kruss drop shape analyzer (DSA25) with an automatic liquid dispenser. The contact angles were measured using a 5 µL water droplet at four locations on each sample. Field emission scanning electron microscope (FESEM) images were taken using a Carl

Zeiss FESEM. A dynamic light scattering (DLS) study was conducted using a Zetasizer Nano ZS90 instrument (ZEN3690). Fourier transform infrared-attenuated total reflectance (FTIR-ATR) spectra were recorded using a Perkin Elmer instrument at ambient conditions. The samples were sputtered with gold before the FESEM analysis. The photographs were captured using a Canon Power Shot SX420 IS digital camera. Phase contrast and fluorescence microscopy images were recorded using a ZEISS Axio Vert.A1 inverted microscope. Solid state fluorescence spectra was recorded in Perkin-Elmer lamda 750 spectrophotometer. Milli-Q grade water was used for all experiments.

### **Preparation of functionalizable porous coating**

The reactive porous polymeric coating was prepared via the spray deposition of reactive nano complex dispersions on various substrates, i.e., microscopic glass slide, aluminum foil, plastic, paper, and wood. The first step involved the preparation of the reactive nano complex solution in heptanol by mixing 10 mL of 5Acl (1.3 g/10 mL) and 3 mL of BPEI (0.5 g/10 mL) in a spraying bottle and shaking vigorously for 5 min until the solution becomes turbid, indicating the formation of the nanocomplex. Next, the nano-complex dispersion (13 mL) was uniformly spray deposited onto the selected substrates over an area of 130 cm<sup>2</sup> from a distance of 10 cm. After the deposition, the coated substrates were dried in air overnight, followed by washing with methanol.

### **Post-functionalization of reactive coating with small molecules**

The reactive porous polymeric coatings were modified further by post-functionalization with various small molecules containing different functional groups, i.e., aldehyde, primary amine, and acrylate functional groups. In the post-functionalization treatment, the coatings were individually placed in the solution containing the desired small molecules for 12 h (5 mg/mL of ODA in THF; 80 mg/mL of HA and Glu in water). Afterward, the coatings were thoroughly washed with ethanol and dried in air.

### **Fabrication of different patterned interfaces**

The prepared hydrophobic reactive porous coating was first exposed to an HA aqueous solution to create hydrophilic patterning on the coating. After drying, the patterned coating was washed repeatedly with ethanol to remove excess reactants. Next, the coating was placed in a THF solution containing ODA overnight, followed by rinsing thoroughly with THF to remove excess ODA. This successive modification of the prepared coating with HA and ODA generates a patterned interface comprising adhesive and nonadhesive superhydrophobicity, respectively. The same procedure was followed to prepare a UV active patterned interface that also displays a pattern of adhesive-nonadhesive superhydrophobicity following the spatially selective modification of the reactive porous coating with Glu instead of HA before treatment with ODA.

Moreover, before post-modification with ODA, the spatially selective modification of the same reactive coating with glucamine instead of HA yielded patterned interfaces with two extremes of wettability (superhydrophilicity and superhydrophobicity). The spatially selective glucamine modification provided a hydrophilic region, and the ODA treatment provided the superhydrophobic regions.

For the QR code-printed patterned interfaces, aluminum foil was used as the substrate. The same procedure discussed above was followed to obtain patterned interfaces coated on aluminum foil. Next, the QR code showing "IITG" was printed on the aluminum foil-supported patterned interface using a laser printer.

### **Particle size analysis**

The growth and size distributions of the nanocomplexes of the reaction mixture of 5-Acl and BPEI in heptanol and ethanol were characterized with DLS. In order to determine the size of the nanocomplexes

formed as the reaction progressed, the reaction mixture of 5-Acl and BPEI at different times was diluted 200 times in ethanol. For every solution, at least 6 measurements were recorded.

### **Self-cleaning performance**

The self-cleaning performance was evaluated using a coating containing deposited dust particles placed under a stream of water. Rolling water droplets over the coating resulted in the collection of the deposited dust particles, showing that the spatially and selectively modified, with either HA@ODA or Glu@ODA, surfaces could be easily cleaned. However, other modifications failed to display the self-cleaning ability (see main text).

### **Convolution neural network architecture**

In this study, we utilized a convolution neural network (CNN) model to automate the authentication of the porous coating fluorescent spots. The CNN model architecture comprised four 2-dimensional convolution layers (Conv2D) with 128, 256, 256, and 512 neurons, respectively; each Conv2D was followed by a rectified linear unit (ReLU) activation function for the elementwise mapping of the input to yield an activated object.<sup>49</sup> Also, a max pooling layer was added after each ReLU activation function for dimension reduction to make the learned object invariant to small-length scale perturbations.<sup>50</sup> A fully dense layer containing 512 neurons was added to the four-layer convolution block, followed by a 50% dropout layer as a regularization mechanism to control overfitting.<sup>51</sup> Afterward, the output from the dropout layer was passed to a dense layer containing 1 neuron with a SoftMax activation function for predicting the probabilities for the binary (Real and Fake) image classification.

### **Training and serving the CNN model**

Micrographs of the porous coating fluorescence spots were converted to grayscale and fed into the CNN model described above. For training the CNN model, we used a validation to training data ratio of 0.2, a

categorical cross-entropy loss function, and an Adam optimizer. The training and validation accuracy and loss results are shown in Fig. 2 and Fig. S4. Afterward, the model was saved, containerized using docker, and deployed on a server to allow for the automated validation of the porous fluorescence coating authenticity.

### **Tissue paper abrasion**

In the tissue paper abrasion test, the superhydrophobic interface with fluorescent dots was rubbed manually with tissue paper in a back-and-forth motion with 100 g of load on top of it for several cycles. Thereafter, fluorescence microscope imaging was performed, and microscopic images of fluorescent dots acquired from this abraded surface were used further for machine learning study.

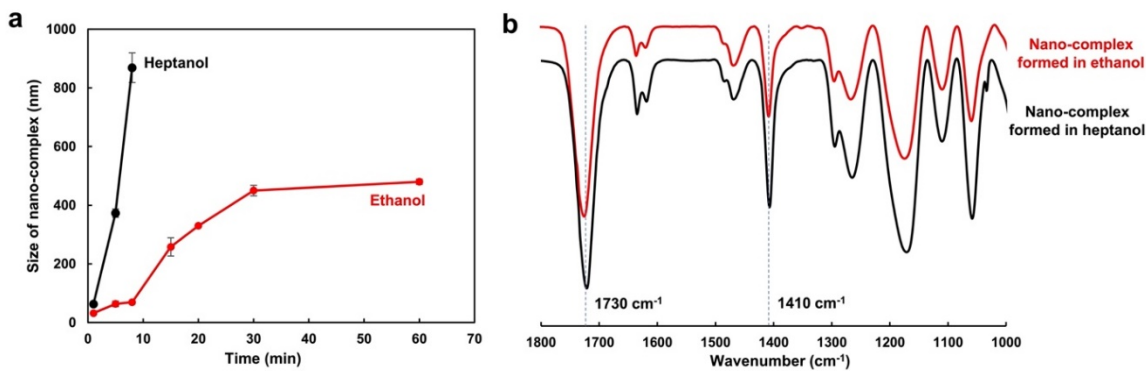


**Figure S1.** a) Comparison of the growth of BPEI/5-Acl nanocomplexes prepared in ethanol (red) or heptanol (black) using DLS. b) ATR-FTIR spectra of the BPEI/5-Acl nanocomplexes prepared in ethanol (red) and heptanol (black). Characteristic IR peaks at  $1,730\text{ cm}^{-1}$  and  $1,410\text{ cm}^{-1}$  corresponding to the carbonyl stretching of ester groups and the symmetric deformation of the vinylic C–H bonds, respectively, indicating the presence of residual acrylate groups in the reactive nano-complexes.

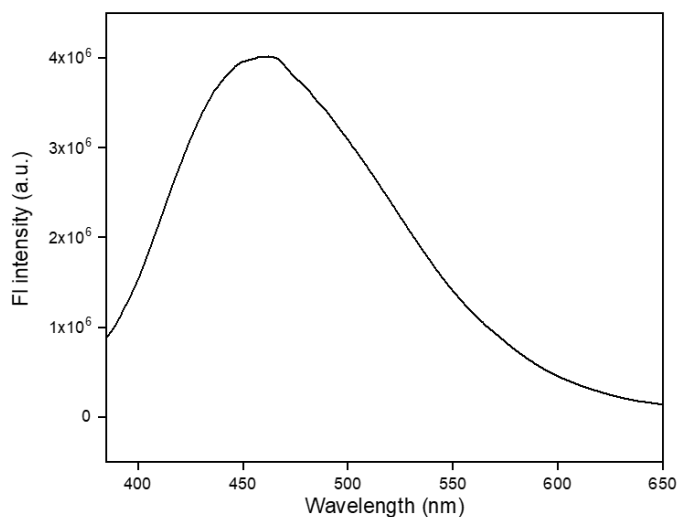


**Figure S2.** Solid state fluorescence spectrum of Glu@ODA modified adhesive superhydrophobic coating.

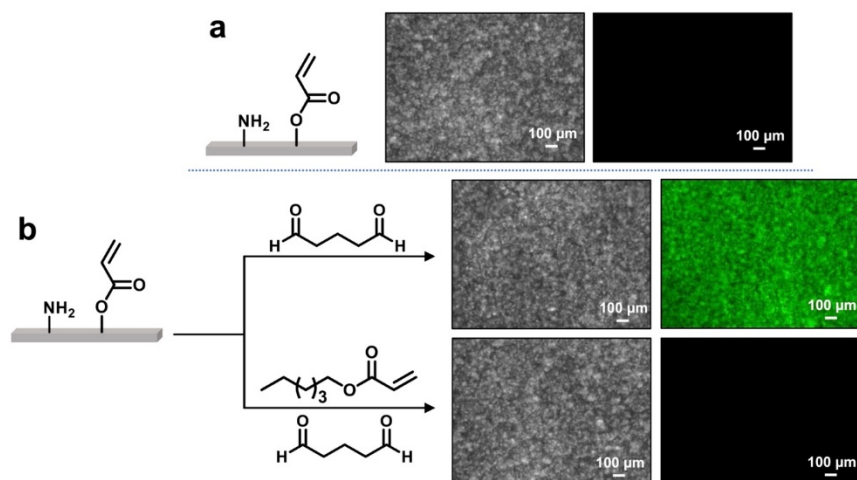


**Figure S3.** a, b) Phase contrast and fluorescence micrographs of functionalizable and porous polymeric coating before (a) and after (b) mono (Glucamine (Glu)) and dual (hexylacrylate (HLA) followed by Glu) post-modification. The inherently non-fluorescent reactive porous coating (a) shows green fluorescence only after successful post-modification with Glu (b). However, the coating does not fluoresce after successive modifications with HLA and Glu, as the available residual amine group is consumed during HLA modification and prevents post-covalent modification with Glu.

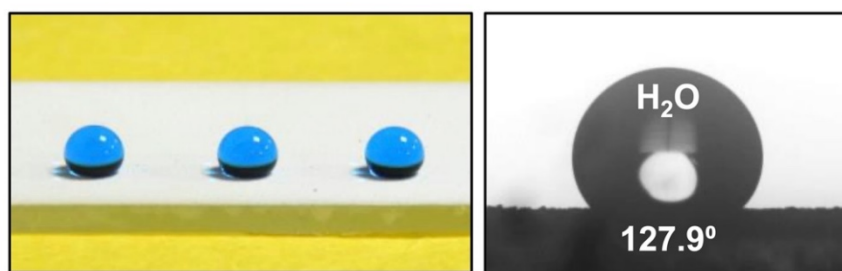


**Figure S4.** Photograph of beaded water droplets (dyed with methylene blue) and the static contact angle measurement on an unmodified porous polymeric coating. The volume of the beaded water droplets was  $12\ \mu\text{L}$  for the photograph and  $5\ \mu\text{L}$  for the contact angle goniometer image.

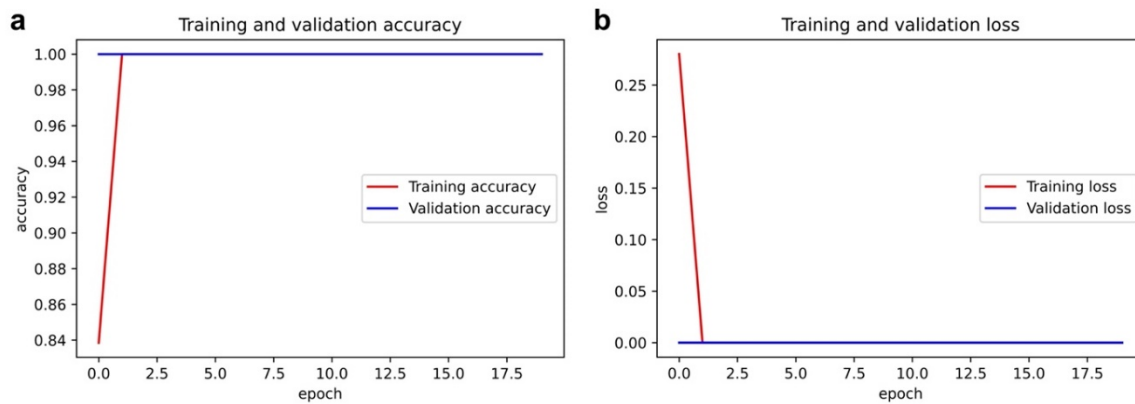


**Figure S5.** a) Training accuracy as a function of the number of training epochs. b) Magnitude of training loss as a function of the number of training epochs.

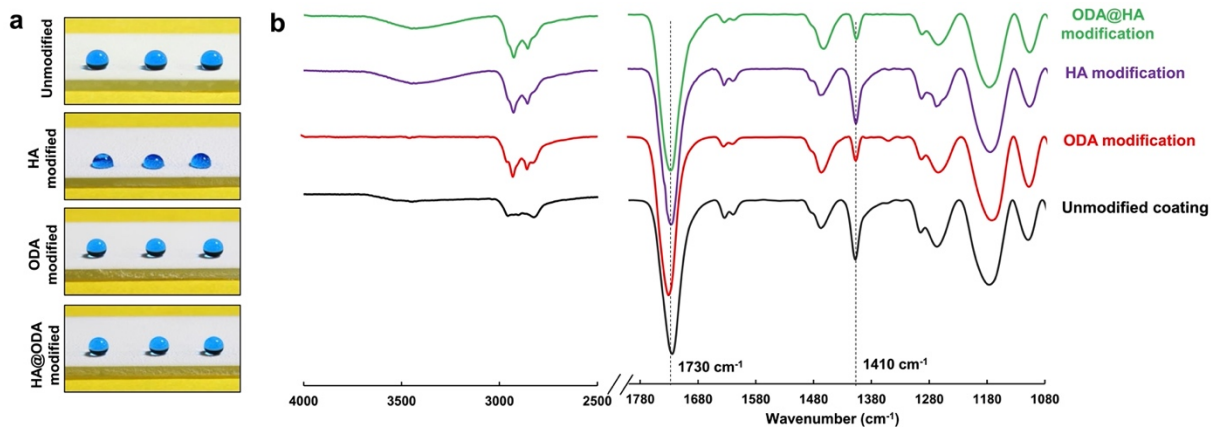


**Figure S6.** Photographs (a) and FTIR-ATR spectra (b) of unmodified (black), HA (purple) modified, ODA (red) modified, and HA@ODA (green) modified porous polymeric coatings. The FTIR-ATR spectra reveal changes in the intensity of certain infrared (IR) peaks after the modification process. After modifying with ODA, the intensity of the IR peak at  $1,410\text{ cm}^{-1}$ , associated with vinylic C–H bonds, decreased significantly. However, modifying with HA resulted in the appearance of an IR peak at  $3,400\text{ cm}^{-1}$ , associated with O–H stretching arising from the association of the HA hydroxyl group to the postmodified coating. In contrast, the characteristic IR signature for the symmetric deformation of the vinylic C–H bond at  $1,410\text{ cm}^{-1}$  remained unchanged. Dual modification with both HA and ODA caused the appearance of the IR peak at  $3,400\text{ cm}^{-1}$  and the decrease in the intensity of the IR peak at  $1,410\text{ cm}^{-1}$ . These changes indicate that the modification process was successful and altered the properties of the porous polymeric coating.

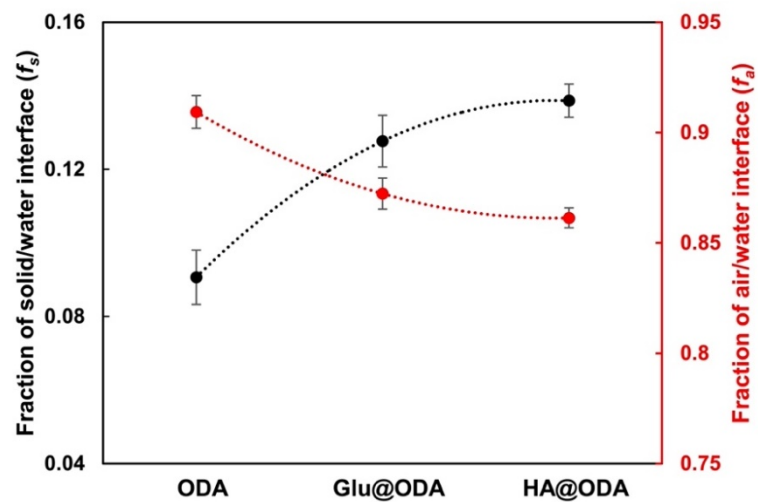


**Figure S7.** The fraction of the contact area of the solid-beaded aqueous phase ( $f_s$ ) and the air-water ( $f_a$ ) interface of the porous polymeric coating after the association of selected mono-functionalization (ODA modification) and two dual modifications of either Glu@ODA or HA@ODA. The figure illustrates how the different modifications affect the contact area of the coating.

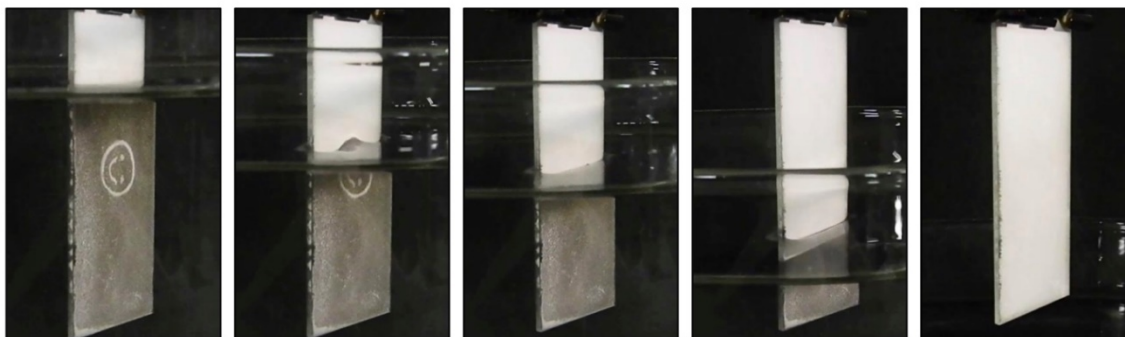


**Figure S8.** Sequential photographs revealing the immediate disappearance of the smiley patterned interface (created through spatially selective chemical modifications with HA@ ODA) when it is removed from the aqueous phase to the air.

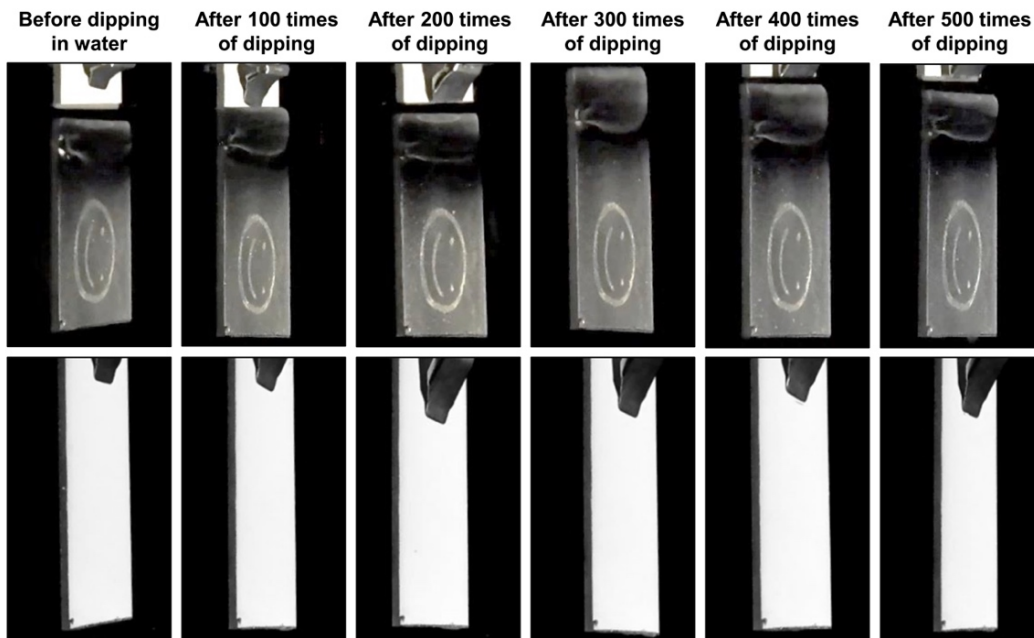


**Figure S9.** Photographs illustrating the durability of the smiley patterned interface after repeated dipping into water.

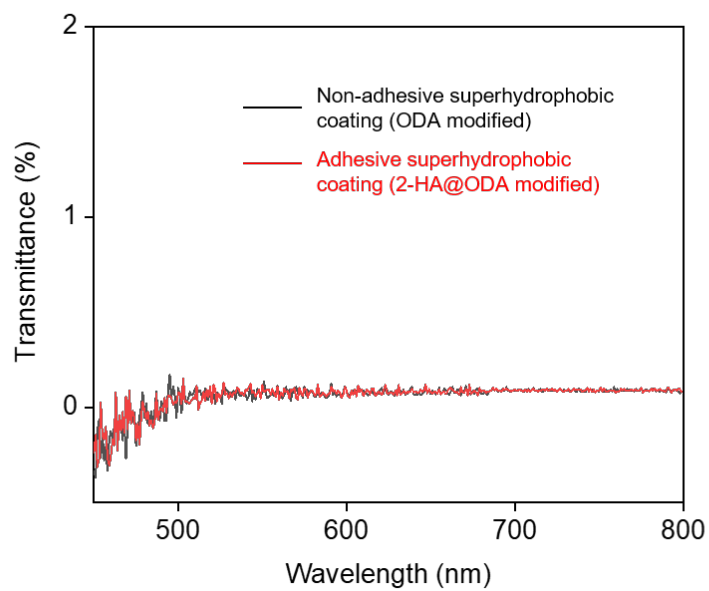


**Figure S10.** Transmittance spectra of non-adhesive (ODA modified) and adhesive (2-HA@ODA modified) superhydrophobic coating.

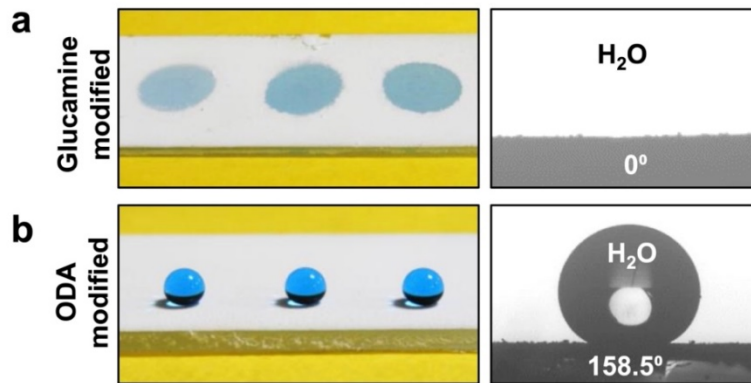


**Figure S11.** a, b) Photographs and contact angle goniometer images of beaded water droplets on the coating after separate post-chemical functionalization with glucamine (a) and ODA (b).

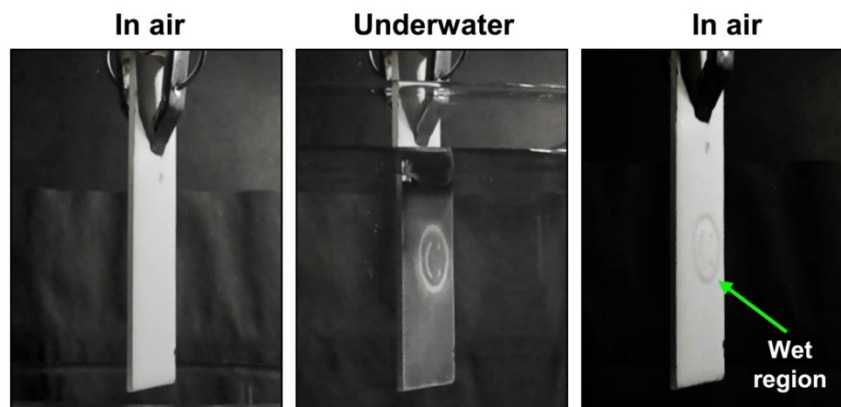


**Figure S12.** Photographs of the smiley patterned interface obtained through the ODA and ODA@glucamine modifications in the air (before submerging it), submerged, and after removing it from the water. The smiley pattern remains visible to the naked eye even after the coating is removed from the water because of the infiltration of water in the hydrophilic smiley patterned region.

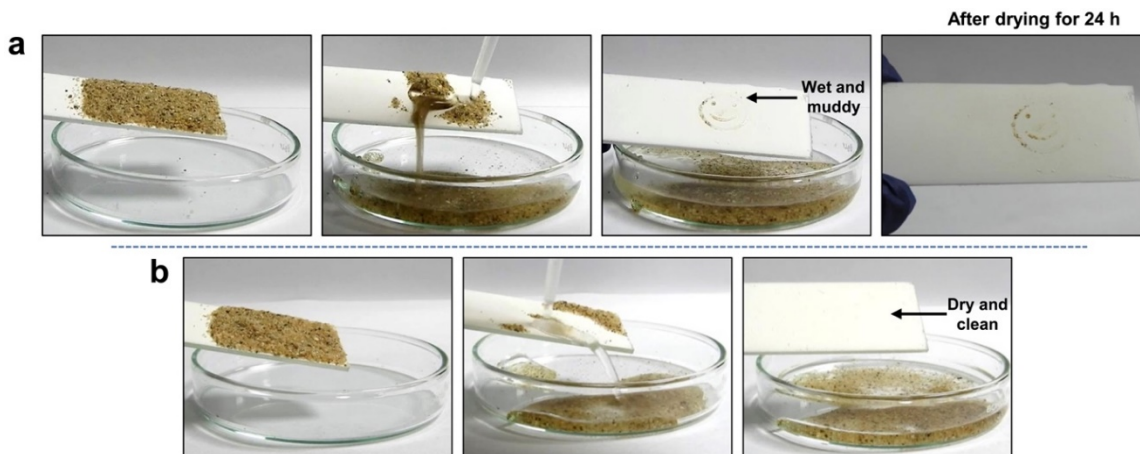


**Figure S13.** Photographs depicting the self-cleaning performance of the smiley patterned interface developed through selective and successive chemical modifications with glucamine@ODA (a) and HA@ODA (b).

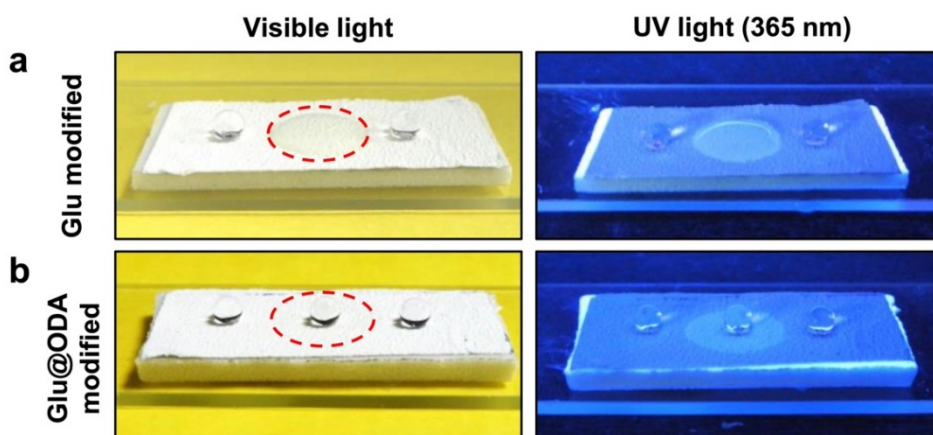


**Figure S14.** Photographs depicting the superhydrophilic fluorescent patterned region on the hydrophobic porous polymeric coating on aluminium foil that was created through selective chemical modification with Glu (red dashed region; a), while the dual chemical modification with Glu and ODA (red dashed region; b) provided an adhesive superhydrophobic fluorescent patterned region on the non-adhesive (ODA treated) region of the superhydrophobic polymeric coating. This is evident from the digital images under visible and UV light (365 nm) in the bottom panel. The volume of the beaded water droplets was 12  $\mu\text{L}$ .

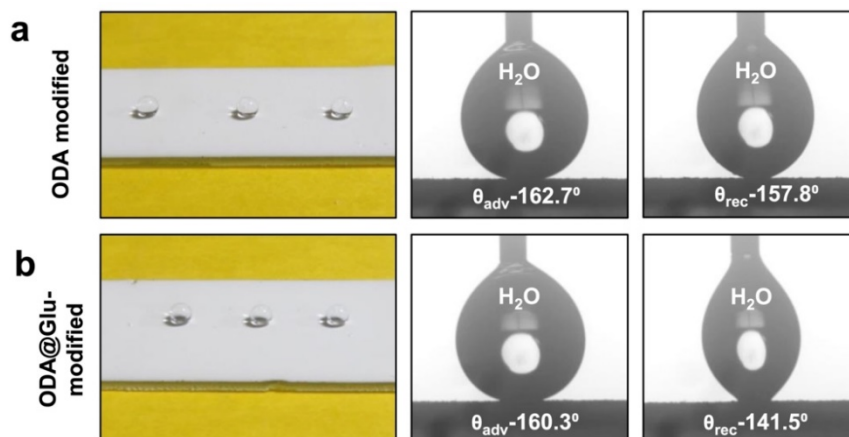


**Figure S15.** Photographs and dynamic (advancing and receding) contact angle images of beaded water droplets on mono (ODA; a) and dual (Glu@ODA; b) modified porous polymeric coatings. The volume of the beaded water droplets was 12  $\mu\text{L}$  in the photographs and 5  $\mu\text{L}$  in the contact angle goniometer images.

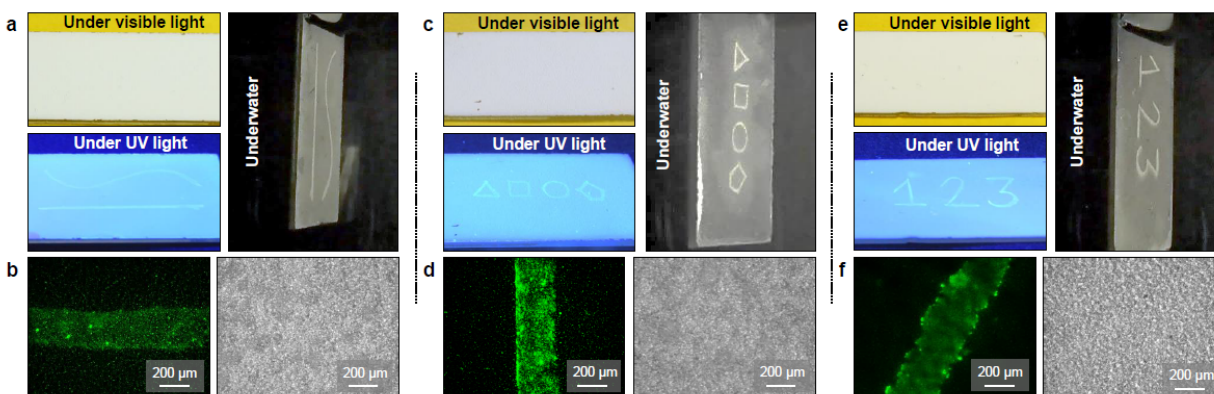


**Figure S16.** a) Photographs showing the appearance of straight- and curved-line patterns (Glu@ODA modified) of micrometre-sized width upon submerging the coating underwater and under UV light illumination, separately. b) Fluorescence and bright field microscope images of straight-line patterned region of the polymeric coating. c) Photographs showing the appearance of different geometrical patterns (Glu@ODA modified) including triangle, square, circle and pentagon of micrometre-sized width upon submerging the coating underwater and under UV light illumination, separately. d) Fluorescence and bright field microscope images of the square patterned region of the polymeric coating. e) Photographs

showing the appearance of numbers (Glu@ODA modified) including 1, 2, and 3 of micrometre-sized width upon submerging the coating underwater and under UV light illumination, separately. f) Fluorescence and bright field microscope images of the number 2 patterned region of the polymeric coating.

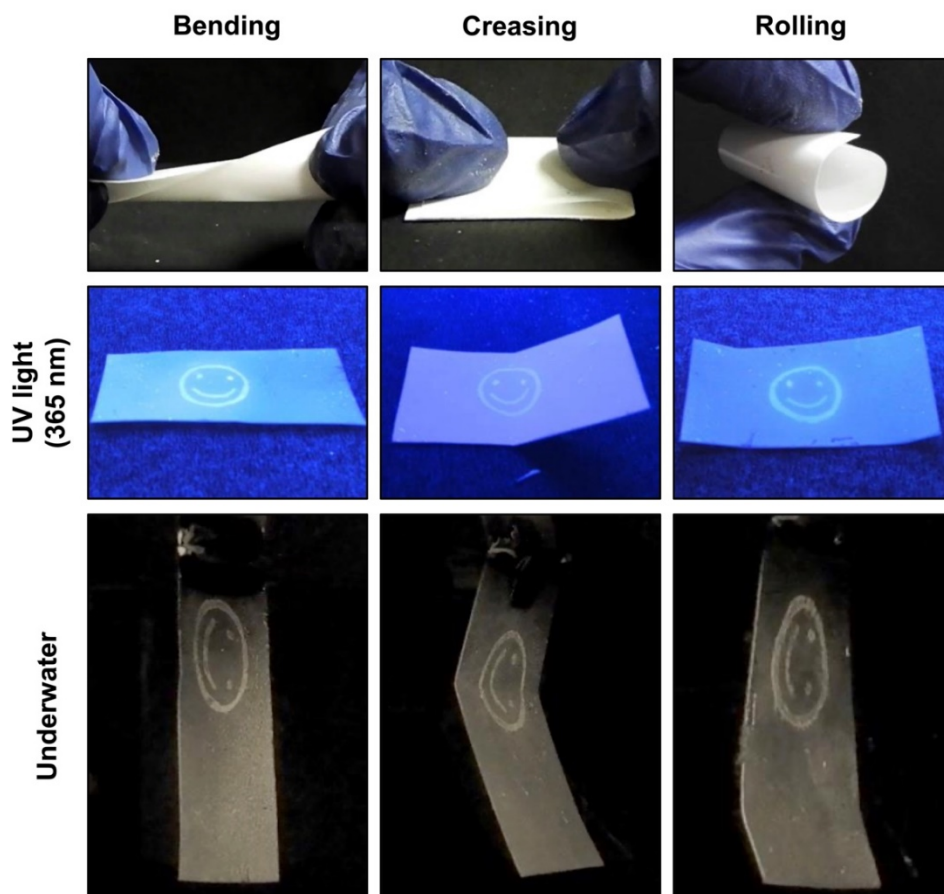


**Figure S17.** Photographs showing the effect of bending, creasing, and rolling on the smiley patterned coating on a flexible plastic substrate.

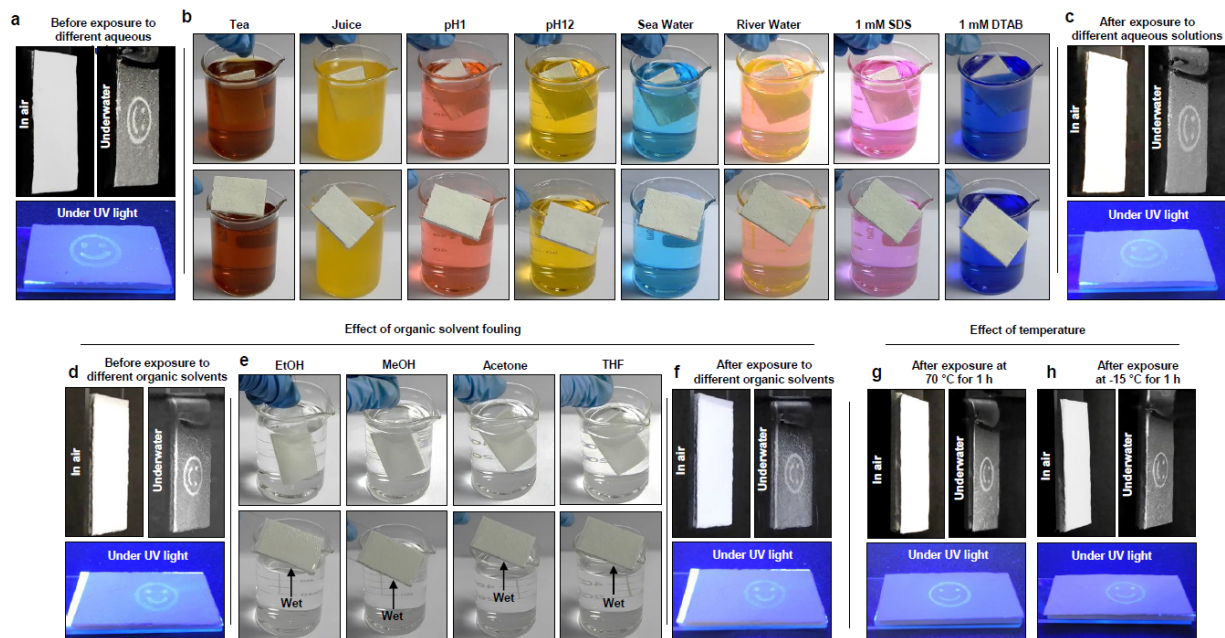


**Figure S18.** a) Photographs showing the appearance of a smiley pattern (Glu@ODA modified) upon submerging the coating underwater and upon irradiation with UV light, separately before exposure to different contaminated aqueous solutions. b) Photographs demonstrating the results of dipping the Glu@ODA patterned polymeric coating in various aqueous solutions, including tea, juice, pH 1, pH 12, saltwater, river water, 1mM SDS, and 1mM DTAB. c) Photographs showing the appearance of a smiley pattern (Glu@ODA modified) upon submerging the coating underwater and upon irradiation with UV light, separately even after exposure to these different contaminated aqueous solutions. d) Photographs showing the appearance of a smiley pattern (Glu@ODA modified) upon submerging the coating underwater and upon irradiation with UV light, separately before exposure to different organic solvents. e) Photographs demonstrating the wetting of Glu@ODA patterned polymeric coating after dipping in ethanol (EtOH), methanol (MeOH), acetone, and tetrahydrofuran (THF). f) Photographs showing the appearance of a smiley pattern (Glu@ODA modified) upon submerging the coating underwater and upon irradiation with UV light, separately even after exposure to different organic solvents. g, h) Photographs showing the appearance of a smiley pattern (Glu@ODA modified) upon submerging the coating

underwater and upon irradiation with UV light, separately even after exposure to extreme temperatures for 1h including 70 °C (g) and -15 °C (h).

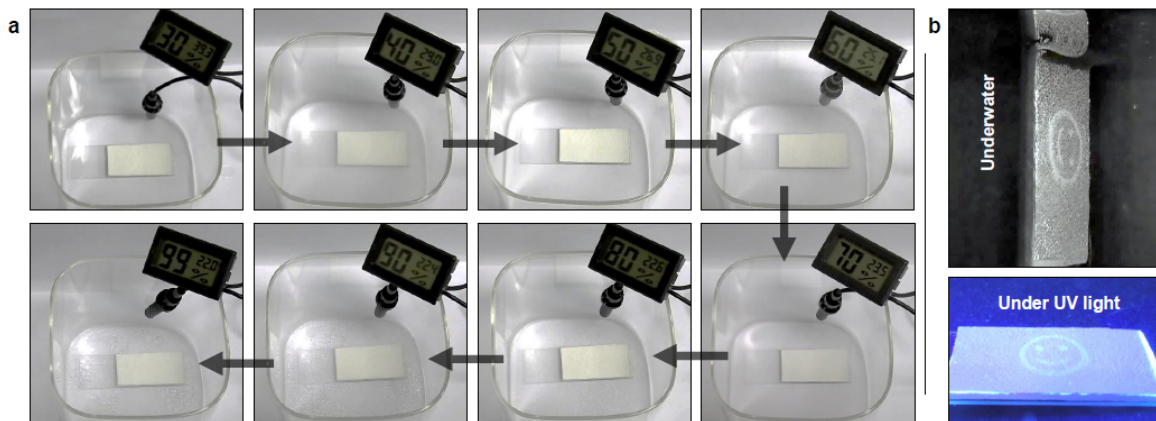


**Figure S19.** a) Photographs demonstrating the effect of different relative humidity on Glu@ODA modified smiley patterned polymeric coating. b) Photographs showing the appearance of a smiley pattern both underwater and under UV light after exposing the polymeric coating to different relative humidity.

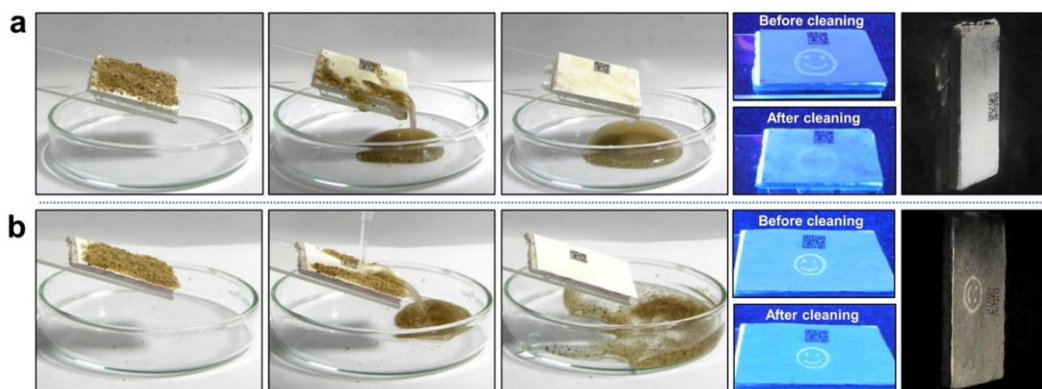


**Figure S20.** Photographs comparing the self-cleaning performance of the deposited dust particles on the smiley patterned interface after Glu modification (a) and dual chemical modifications with Glu@ODA (b).

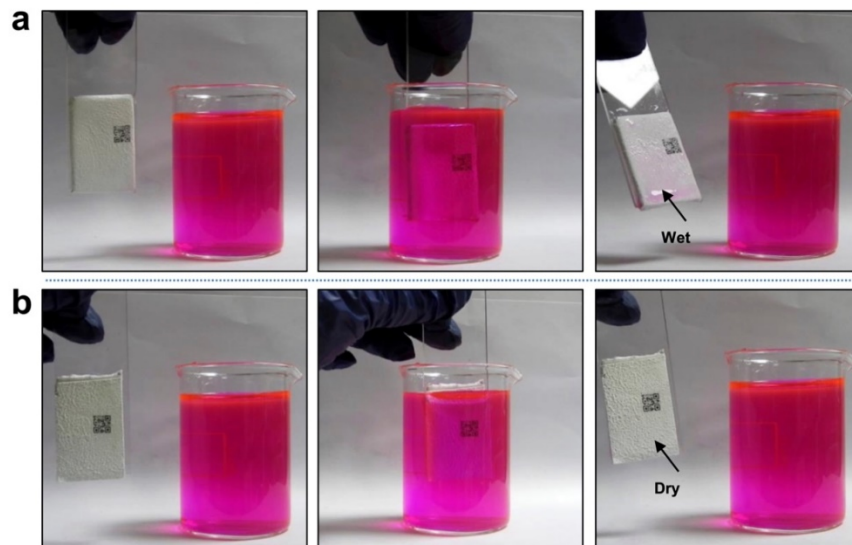


**Figure S21.** Digital images depicting the effect of dyed (Rhodamine B) aqueous exposure on the smiley patterned interface after Glu modification (a) and after dual chemical modifications with Glu@ODA (b).

## **Supplementary movies**

**Movie S1: Pattern decoding upon submerging underwater.** A smiley pattern created through ODA and HA@ODA modification remained invisible in air but appeared on submerging underwater. The pattern instantly disappeared upon bringing it out from the aqueous phase. The water phase failed to wet the pattern interface due to association of extreme water repellence.

**Movie S2: Pattern decoding in the presence of a beaded water droplet.** A smiley pattern created through ODA and HA@ODA modification only appeared in air on beading a water droplet on it. The pattern instantly disappeared on displacement of the beaded water droplet on the prepared pattern interface. During this process, no fouling of the pattern interface was noted because of the association of extreme water repellence.